Evanescent-Mode Ridged Waveguide Bandpass Filters With Improved Performance

Anatoly Kirilenko, *Senior Member, IEEE*, Leonid Rud, *Member, IEEE*, Vladimir Tkachenko, and Dmitry Kulik

***Abstract*—New types of evanescent-mode bandpass filters based on the ridged waveguide sections are considered. Insertion of additional inductive strips between the ridge sections enables one to reduce the longitudinal filter size, increase the cross section of the ridged waveguide housing, and achieve a sufficient improvement of stopband characteristics. Results of designing the millimeter-wave filters and comparison with the measured data are presented.**

***Index Terms*—Bandpass filter, filter design, ridged waveguide.**

I. Introduction

THE well-known advantages of the evanescent-mode ridged waveguide bandpass filters stimulated the development of various full-wave models for their design [1]–[6]. Usually, a filter housing is made on basis of a below-cutoff rectangular waveguide of the standard cross section [1]–[4]. To extend the high-frequency stopband, a smaller filter housing width has to be chosen because the stopband width is limited, as a rule, by parasitic spikes arising due to the half-wave resonances in the notches becoming above-cutoff ones at high frequencies. Such a forced reduction of the housing width and, as consequence, using the narrower ridge gaps may lead to an increase in ohmic loss and a complication in the fabrication, for example, of millimeter-wave filters.

The potentials of two new filter configurations of narrow and moderate bandwidths are considered in the present paper to solve the problem of an ohmic loss decrease and stopband extension. Both of them are based on the constant-gap double-ridge waveguide sections and have no input/output transformers, as in [3]. The first-type filter differs from conventional ones by enlarged cross section of the below-cutoff filter housing, the height of which coincides with the height of input/output waveguide, as shown in Fig. 1(a). The possibility to operate with an increased ridge gap is the main feature of such filters. The second-type filter has additional inductive strips inserted to notches between ridge resonators [see Fig. 1(b)]. The strips have the same thickness as the ridges so that the resulting filter topology presents an all-metal E-plane insert placed symmetrically into the filter housing. The length of strips is a constant value s, and they are symmetrically placed between two resonator sections so that $l_i^{(1)} = l_i^{(2)} = l_i$ if $i = 1, \ldots, N-1$, where N is the number of filter sections. For both filter configurations, parameters $l_0 = l_N$ are the lengths of the first and last strip-free notches.

Manuscript received September 15, 2000.

The authors are with the Institute of Radiophysics and Electronics, National Academy of Sciences of Ukraine, Kharkov 61085, Ukraine.

Publisher Item Identifier S 0018-9480(02)04062-0.

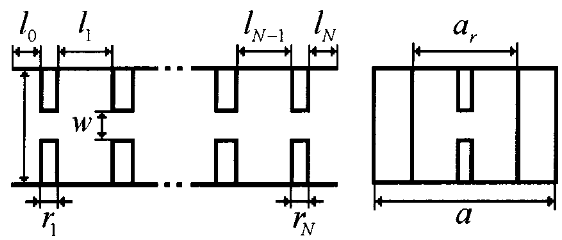

(a)

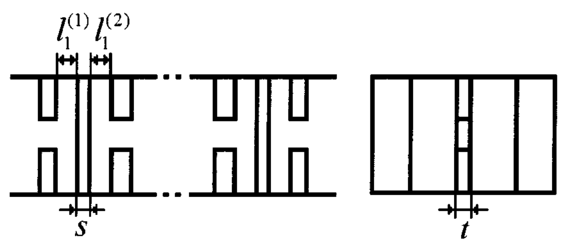

(b)

Fig. 1. Longitudinal and front views of bandpass filters under consideration. (a) Filters with simple-notch elements. (b) Filters with notch–strip–notch elements.

II. Design Considerations

We used the mode-matching technique to build exact numerical models of the rectangular-to-rectangular and rectangular-to-ridged waveguide junctions as filter key elements. The full-wave S-matrix of a rectangular waveguide bifurcation was calculated in accordance with the technique described in [7] and by using the solutions of the Neumann and Dirichlet scalar problems about a parallel-plate waveguide bifurcation [8]. The latter solutions were also applied to develop an algorithm for computing the ridged waveguide TE- and TM-mode bases by the transverse-resonance technique. The analysis of combined filter components, as well as the analysis of a filter as a whole, was performed by the generalized S-matrix technique. The improved procedure of the prototype filter synthesis [6] was used to obtain an initial filter configuration needed to feed the optimization procedure. The latter was based on the multiparametric gradient approach and worked in some stages with different goal functions. At the first stage, a special emphasis was put on the filter response to satisfy the specified skirt selectivity and width of the passband. At the other stages, the required level of passband return loss was reached.

The influence of strips on forming the desired characteristics of separate ridge resonators coupled with semi-infinite ridge waveguides through the notch–strip–notch elements has been studied previously. The opportunity of an essential reduction

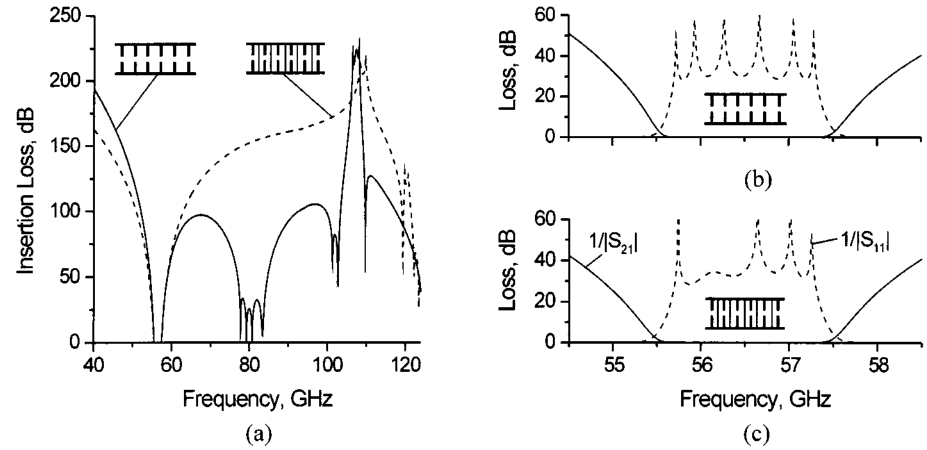

Fig. 2. Computed frequency responses of the designed six-pole narrow-band filters. (a) Responses within a broad frequency range. (b) Simple-notch filter response within the specified range. (c) Notch–strip–notch filter response within the specified range. WR-19 input/output waveguide, ridge thickness $t = 0.2$ mm, ridge gapwidth $w = 0.787$ mm. Other filters dimensions (in millimeters): simple-notch filter—$a_r \times b_r = 2.228 \times 2.387, l_0 = l_6 = 0.979, l_1 = l_5 = 3.526, l_2 = l_4 = 3.750, l_3 = 3.835, r_1 = r_6 = 0.237, r_2 = r_5 = 0.233, r_3 = r_4 = 0.231$; notch–strip–notch filter—$a_r \times b_r = 2.387 \times 2.387, s = 0.2, l_0 = l_6 = 0.984, l_1 = l_5 = 0.486, l_2 = l_4 = 0.676, l_3 = 0.731, r_1 = r_6 = 0.489, r_2 = r_5 = 0.751, r_3 = r_4 = 0.621$.

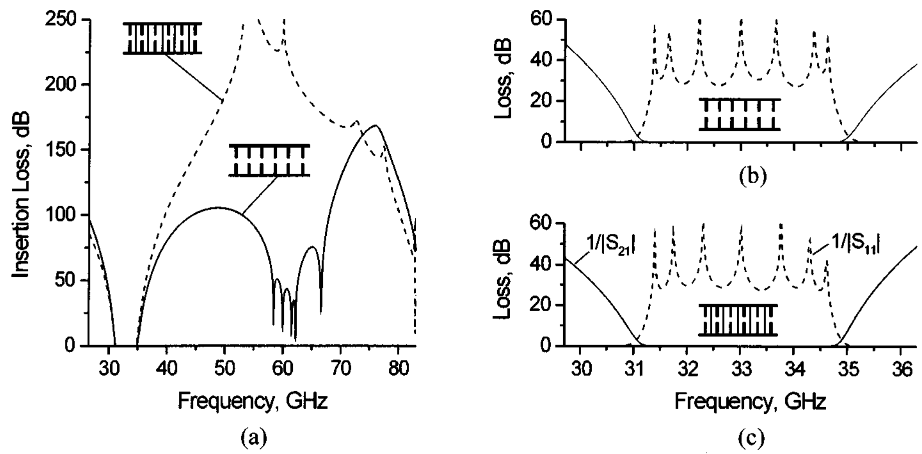

Fig. 3. Computed frequency responses of the designed seven-pole filters of a moderate bandwidth. (a) Responses within a broad frequency range. (b) Simple-notch filter response within the specified range. (c) Notch–strip–notch filter response within the specified range. WR-28 input/output waveguide, ridge thickness $t = 0.2$ mm. Other filters dimensions (in millimeters): simple-notch filter—$a_r \times b_r = 3.556 \times 3.556, w = 0.956, l_0 = l_7 = 0.212, l_1 = l_6 = 2.474, l_2 = l_5 = 2.995, l_3 = l_4 = 3.160, r_1 = r_7 = 0.749, r_2 = r_6 = 0.965, r_3 = r_5 = 0.932, r_4 = 0.928$; notch–strip–notch filter—$a_r \times b_r = 4.0 \times 3.556, w = 0.556, s = 0.3, l_0 = l_7 = 0.250, l_1 = l_6 = 0.512, l_2 = l_5 = 0.639, l_3 = l_4 = 0.709, r_1 = r_7 = 0.366, r_2 = r_6 = 0.746, r_3 = r_5 = 0.661, r_4 = 0.633$.

of the lengths of below-cutoff notches by using the strips is an obvious fact because the latter are strongly scattering obstacles. Numerical studies have shown that, in fact, the use of the notch–strip–notch coupling elements increases a ridge resonator length in comparison to the case of a ridge resonator with the conventional simple-notch coupling elements. This is caused by an additional inductance introduced by the strips to a resonator equivalent circuit. Independently of the strip size, the overall length of the resonator structure bounded by the notch–strip–notch elements is always smaller than that of a structure with the same properties, but based on the simple-notch elements. At first glance, the observed reduction of the structure length is a positive factor, however, it has a negative effect as well. The matter is that the larger the resonator length, the lower the frequency at which the parasitic spike corresponding to the ordinary half-wave resonance can arise. As a result, it reduces the width of the high-frequency stopband. That is why it is better to choose the strip length as small as possible from the viewpoint of requirements on the rigidity of the filter all-metal insert or the technology of its fabrication.

III. Numerical and Measured Results

Now we demonstrate the opportunities offered by the developed design algorithm and consider the examples of narrow and moderate bandwidth filters. Comparative analysis of the characteristics of narrow-band filters with the simple-notch (filter 1) and notch–strip–notch (filter 2) elements can be carried out with the aid of responses shown in Fig. 2. As the specification on filter design, the following parameters were given: the passband edge frequencies of $f_b = 55.7$ and $f_c = 57.3$ GHz, insertion loss ripples within the passband of $L_r \leq 0.01$ dB, the suppression of $L_{a,d} = 40$ dB at the stopband edge frequencies $f_a = 54.5$, and $f_d = 58.5$ GHz. This specification is similar to the one formulated in [4, Fig. 11], where the filter

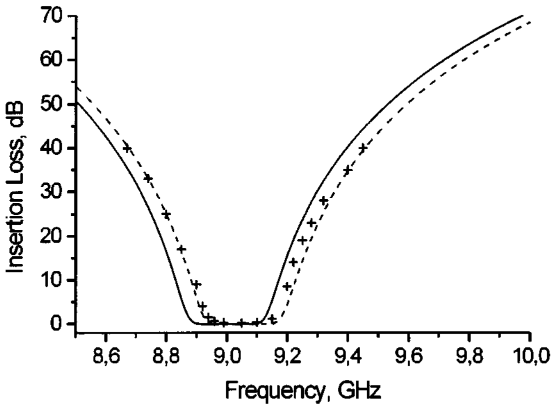

Fig. 4. Computed response of the designed 2% bandwidth filter (solid curve). Response calculated with the measured dimensions of the fabricated filter (dashed curve). Crosses mark measured data. Input/output waveguide of 23 × 10 mm. Designed filter dimensions (in millimeters): $a_r \times b_r = 11.5 \times 10$, $t = 2$, $w = 1.8$, $s = 0.3$, $l_0 = l_4 = 4.104$, $l_1 = l_3 = 3.595$, $l_4 = 4.063$, $r_1 = r_4 = 3.072$, $r_2 = r_3 = 4.061$. Fabricated filter dimensions: $a_r \times b_r = 11.47 \times 10$, $t = 1.97$, $w = 1.82$, $s = 0.28$, $l_0 = 4.12$, $l_1 = 3.625$, $l_2 = 4.075$, $l_3 = 3.62$, $l_4 = 4.08$, $r_1 = 3.05$, $r_2 = 4.045$, $r_3 = 4.04$, $r_4 = 3.05$.

with different ridge gapwidths $w_i \approx 0.2$–0.23 mm of the resonator sections was designed. Below-cutoff ridged waveguide sections of $a_r \times b_r = 2.228 \times 0.902$ mm and different gaps around $w_i \approx 0.9$ mm were considered as the filter elements in [4]. In contrast to the filter designed in [4], the filters in Fig. 2 have the constant ridge width $w = 0.787$ mm and housings, the heights of which are the same as of the input/output waveguides. As one can see, filter 2 has the advantage over filter 1 due to essentially expanded high-frequency stopband [see Fig. 2(a)] with comparable characteristics within the specified frequency range [compare responses in Fig. 2(b) and (c)]. Moreover, filter 2 has a shorter overall length of $l_\Sigma \approx 13.3$ mm in comparison with $l_\Sigma \approx 21.2$ mm for filter 1 and with $l_\Sigma \approx 20$ mm for the filter designed in [4]. It should be noted that the insertion loss responses were calculated as

$$L(f) = -10 \log \sum_{m=1}^{M} P_m(f)$$

where P_m is the relative power of the mth mode and M is the number of modes propagating in the filter output port at the given frequency f ($m = 1$ corresponds to the dominant TE_{10} mode).

Fig. 3 shows the results of designing the 10%-bandwidth filters in the WR-28 rectangular waveguide according to the following specification: $f_a = 29.7$, $f_b = 31.35$, $f_c = 34.65$, and $f_d = 36.3$ GHz, $L_{a,d} = 40$, and $L_r = 0.01$ dB. As for narrow-band filters, the improved stopband performance is realized in filter 2 with the notch–strip–notch elements. This filter has a smaller ridge gapwidth in comparison with filter 1. The lengths of filters 1 and 2 are $l_\Sigma \approx 23.9$ and $l_\Sigma \approx 13.9$ mm, respectively.

To verify the developed design procedure, a four-pole filter with the notch–strip–notch elements has been fabricated and measured. The specification on the filter design was $f_a = 8.64$, $f_b = 8.91$, $f_c = 9.09$, and $f_d = 9.36$ GHz and $L_{a,d} = 40$ and $L_r = 0.01$ dB. The designed configuration has the overall length of $l_\Sigma \approx 45$ mm and provides the calculated upper stopband characteristic with $L > 40$ dB up to 24.7 GHz. The comparison of theoretical and measured data is shown in Fig. 4. As one can see, the results are in a good agreement, except of the passband location. The observed difference is caused mainly by the inaccuracy in the gapwidth and resonator length fabrication. The wider gap and shorter resonator sections led to the desired small high-frequency shift of the response of the fabricated filter. In addition to ohmic loss, nonsymmetry of the actual filter configuration is a reason for an increased level of the passband insertion loss (the measured value was $L_{r,\max} \approx 0.6$ dB instead of the specified one $L_r = 0.01$ dB).

IV. Conclusion

The above-presented results show that the filter configurations with increased in height below-cutoff housings and wide ridge gaps allow obtaining the characteristics similar to the ones of conventional evanescent-mode filters. One can assume that such housings and ridge gaps will reduce ohmic loss essentially. An insertion of additional inductive strips into notches leads to filter configurations with improved stopband performance, smaller longitudinal size, and larger cross section of the filter housing.

References

[1] J. Bornemann and F. Arndt, "Rigorous design of evanescent mode E-plane finned waveguide bandpass filters," in *IEEE MTT-S Int. Microwave Symp. Dig.*, 1989, pp. 603–606.

[2] ——, "Transverse resonance, standing wave, and resonator formulations of the ridge waveguide eigenvalue problem and its application to the design of E-plane finned waveguide filters," *IEEE Trans. Microwave Theory Tech.*, vol. 38, pp. 1104–1113, Aug. 1990.

[3] J.-C. Nanan, J. W. Tao, H. Baudrandt, B. Theron, and S. Vigneron, "A two-step synthesis of broad-band ridged waveguide bandpass filters with improved performances," *IEEE Trans. Microwave Theory Tech.*, vol. 39, pp. 2192–2197, Dec. 1991.

[4] J. Bornemann and F. Arndt, "Modal S-matrix design of metal finned waveguide components and its application to transformers and filters," *IEEE Trans. Microwave Theory Tech.*, vol. 40, pp. 1528–1537, July 1992.

[5] Y. Rong, K. A. Zaki, J. Gipprich, M. Hageman, and D. Stevens, "LTCC wide-band ridge-waveguide bandpass filters," *IEEE Trans. Microwave Theory Tech.*, vol. 47, pp. 1836–1840, Sept. 1999.

[6] A. Kirilenko, L. Rud, V. Tkachenko, and D. Kulik, "Design of bandpass and lowpass evanescent-mode filters on ridged waveguides," in *Proc. 29th Eur. Microwave Conf.*, vol. 3, 1999, pp. 239–242.

[7] T. Vasilyeva, A. Kirilenko, L. Rud, and V. Tkachenko, "Calculation of full-wave S-matrices of monoaxially uniform (2D) elements in rectangular waveguides," in *Proc. Int. Methods Electromagn. Theory Conf.*, Kharkov, 1998, pp. 399–401.

[8] L. Rud, "An efficient algorithm for analyzing a waveguide bifurcated by a thin semi-infinite plate and its application to the design of millimeter-wave bandpass filters," *Telecommun. Radio Eng.*, vol. 51, no. 2–3, pp. 112–118, 1997.

Anatoly Kirilenko (M'95–SM'99) was born in Tambov, Russia, in 1943. He received the Research degree in radiophysics, Ph.D. degree, and D.Sc. degree from the Kharkov State University, Kharkov, Ukraine, in 1965, 1970, and 1980, respectively.

In 1989, he received a Professor title in radiophysics. Since 1981, he has been a Professor with the National Aerospace University, Kharkov, Ukraine. Since 1965, he has been with the Institute of Radiophysics and Electronics, National Academy of Sciences of Ukraine, where he is currently a Head of the Department of Computational Electromagnetics. His research interests are analytical and numerical methods in electromagnetics, resonance phenomena in waveguides and gratings, microwave computer-aided engineering (CAE) and computer-aided design (CAD).

Prof. Kirilenko was the recipient of the 1989 State Prize of Ukraine in the field of science and technology.

Leonid Rud (M'98) was born in the Donetsk region, Ukraine, in 1946. He received the Radiophysics Engineering degree from the Kharkov Institute of Radioelectronics, Kharkov, Ukraine, in 1964, and the Ph.D. and D.Sc. degrees from the Kharkov State University, in 1974 and 1990, respectively.

In 1984, he received a Senior Scientist title in radiophysics. Since 1971, he has been with the Institute of Radiophysics and Electronics, National Academy of Sciences of Ukraine, Kharkov, Ukraine, where he is currently a Leading Scientist with the Department of Computational Electromagnetics. From 1992 to 1996, he was a Professor at the Kharkov State Technical University of Radioelectronics. His research interests include mathematical simulation of wave scattering by waveguide discontinuities, spectral theory of open waveguide resonators, and CAD of waveguide components and devices.

Dr. Rud was the recipient of the 1989 State Prize of Ukraine in the field of science and technology.

Vladimir Tkachenko was born in Lvov, Ukraine, in 1951. He received the Researcher and Ph.D. degrees in radiophysics from the Kharkov State University, Kharkov, Ukraine, in 1973 and 1986, respectively.

From 1973 to 1981, he was with the Low Temperature Physics Institute, National Academy of Sciences of Ukraine, Kharkov, Ukraine, where he was involved with the development of superconductive antennas theory. In 1981, he joined the Institute of Radiophysics and Electronics, National Academy of Sciences of Ukraine, where he is currently a Senior Scientist with the Department of Computational Electromagnetics. From 1991 to 1996, he was an Assistant Professor at the Kharkov State Technical University of Radioelectronics. His research interests are numerical algorithms and software for the design of microwave devices and large-scale modeling systems for waveguide electromagnetics. In 1991, in Russia (then the USSR), one of these systems was recognized as the best software in the area of microwave electronics.

Dmitry Kulik was born in Kharkov, Ukraine, in 1965. He received the Radioelectronics Engineering degree from the Kharkov Aviation Institute, Kharkov, Ukraine, in 1988.

From 1988 to 1993, he was with the Radar Department, from 1993 to 1998, with the Center of Remote Sensing of Earth, and since 1998, with the Department of Computational Electromagnetics, Institute of Radiophysics and Electronics, National Academy of Sciences of Ukraine, Kharkov, Ukraine, where he is currently a Leading Engineer. His research interests are a computer simulation of microwave devices, development of the software for designing waveguide filters, and diplexers.